

УДК 539.23; 559.216.1

## Whispering gallery mode emission from microtube cavity

Y. P. RAKOVICH, K. I. RUSAKOV, A. A. GLADYSHCHUK, S. V. CHUGUNOV,  
J. F. DONEGAN, S. BALAKRISHNAN, Y. GUNCO, T. PEROVA, A. MOORE

In recent years the studies of electromagnetic modes in solid three-dimensional microcavities have been of great interest both for their potential applications and fundamental optical properties. Among others optical emitters with cylindrical or microcapillary dielectric resonators which support whispering gallery modes (WGMs) have gained much interest due to their microscopic size, high quality factor  $Q$  and possibility to achieve low lasing threshold [1-4]. Resonantly enhanced optical response and material compatibility with telecommunication optical fibres make these high- $Q$  microcavities attractive as novel building blocks for photonic devices. The cylindrical cavity format is also compatible with a large variety of sensing modalities such as immunoassay and molecular diagnostic assay [5, 6]. Experimentally, the most widely studied configuration of thin-wall microtube cavities is the microcapillary filled with a highly-luminescent dye solution.[3, 7] The diameter (typically 50-200  $\mu\text{m}$ ) and wall thickness of these microcapillaries can be controlled by the etching of commercially available glass samples in an HF-water solution. The short-distance evanescent field in these microcavities and limited photostability of dye molecules are retarding factors for potential applications. In the small-size regime (diameter  $< 10 \mu\text{m}$ ), semiconductor microdisks of finite height or micropillars have been widely used as a tool to control spontaneous emission and confine photons in three dimensions.[1] The evanescent field in these photonic structures extends a couple of micrometers into the surroundings providing the possibility for efficient coupling to an external photonic device. However fabrication of small ( $< 10 \mu\text{m}$  diameter) high- $Q$  cylindrical semiconductor microcavities involves complex and expensive processes [1, 8].

In this paper, we describe a simple method for fabricating highly-luminescent small aluminosilicate microtubes (MT) of  $\sim 8 \mu\text{m}$  diameter using sol-gel processing and a micro-channel glass membrane as a template. The sharp periodic structure observed in emission spectra originates from strong light confinement of whispering gallery modes (WGMs) in the microtubes. We report on the observation of two related features unique to amplification of spontaneous emission (ASE): a nonlinear behaviour of photoluminescence (PL) intensity under varying optical excitation and a corresponding modification of spontaneous emission rate.

In our fabrication approach, we took advantage of the well developed sol-gel technique[9, 10] combined with the versatility of ordered porous membranes as templates. The  $\text{Si}(\text{OC}_2\text{H}_5)_4$  (tetraethylorthosilicate or TEOS) was first hydrolysed during 1 h at room temperature with a solution of  $\text{H}_2\text{O}$ ,  $\text{C}_2\text{H}_5\text{OH}$  and  $\text{HCl}$  in the molar ratios 1: 1: 0.0027 per mole of  $\text{Si}(\text{OC}_2\text{H}_5)_4$  respectively. Then  $\text{Al}(\text{OC}_4\text{H}_9^{\text{sec}})_3$  was added to this solution and the mixture was stirred for 15 min at  $70^\circ\text{C}$ . The resultant homogenous mixture was hydrolysed by adding the mixed solution of  $\text{H}_2\text{O}$ ,  $\text{C}_2\text{H}_5\text{OH}$  and  $\text{HCl}$  in the molar ratio 4: 1: 0.011 per mole of alkoxide, respectively. Finally, a 30-minute stirring provided the conversion of this sol to  $5\text{Al}_2\text{O}_3 \cdot 95 \text{SiO}_2$  (mol%) aluminosilicate gel. The sol, just before its gelation point was then placed on the top of the micro-channel glass samples (donated by State Optical Institute, St. Petersburg, Russia) and 30 mbar - vacuum assisted filtration resulted in the formation of tubes inside the channels. Following drying at room temperature for 1 day and further annealing at  $500^\circ\text{C}$  for 2 hours, the fabricated MT were isolated by the mechanical destruction of the template (Figure 1).

This thermal treatment regime resulted in highly emissive air-stable samples which display broad-band visible photoluminescence originating from carbon substitutional defects for silicon. An elemental analysis study of the annealed aluminosilicate gel showed carbon and hydrogen content

of 0.32% and of 0.56% respectively. SEM imaging analysis showed that the fabricated MT have an outer diameter of 7-8  $\mu\text{m}$  and an inner diameter of 2.7-3  $\mu\text{m}$ . The maximum length of a single MT was 200  $\mu\text{m}$ .

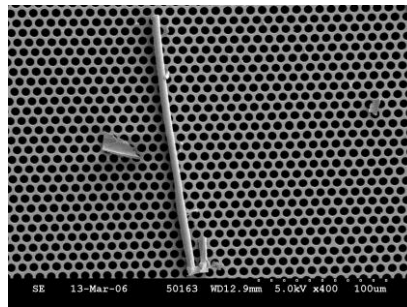


Figure 1. SEM images of aluminosilicate microtubes on the matrix.

The optical spectra of fabricated MT were analyzed by spatially resolved micro-PL at room temperature. The micro-PL spectra from MT were recorded in a backscattering geometry using a RENISHAW micro-Raman system (1800  $\text{mm}^{-1}$  grating,  $> 1 \text{ cm}^{-1}$  spectral resolution) equipped with a notch and a plasma filters and a CCD camera. The spatial resolution, of less than 1  $\mu\text{m}$ , was provided using a microscope with a x100 objective lens and a positioning stage. An  $\text{Ar}^+$  laser (wavelength  $\lambda = 514.5 \text{ nm}$ ) was used as the optical pump source. A polarizer inserted into the optical beam path in front of the detection system was used in the polarization experiments.

When embedded into the matrix, we observe a broad PL band associated with carbon defects in the tube (Figure 2a).

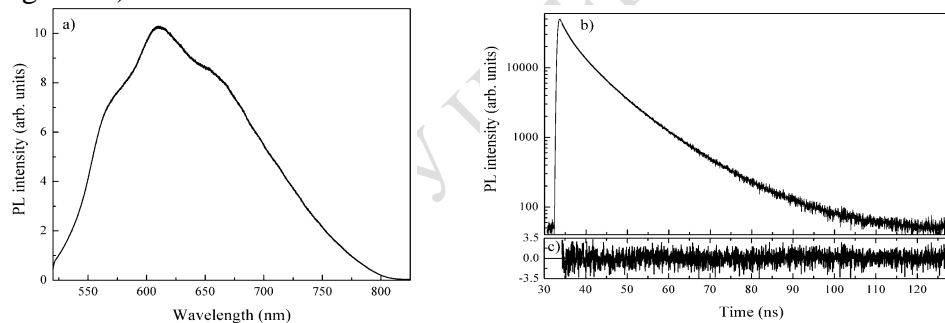


Figure 2. PL spectra (a) and time-dependent PL intensity decay of a single aluminosilicate microtube accommodated in glass micropore (b). Results of three-exponential analysis of decay curves are shown by thick red line with corresponding residual (c).

The PL of a single aluminosilicate MT shows distinct multi-exponential decay. Sum of at least three-exponential functions is required to achieve satisfactory fit to the decay data (Figure 2b) yielding reasonable plot of weighted residuals (Fig. 2c),  $\chi^2$  value 1.1 with corresponding lifetimes in the nanosecond time scale (Table 1).

Table 1.

$\tau_1$ (ns)	$\alpha_1$	$\tau_2$ (ns)	$\alpha_2$	$\tau_3$ (ns)	$\alpha_3$	$\tau_{av}$ (ns)
1.701	0.28	5.391	0.52	11.742	0.20	7.81

In contrast to this broad PL band of the tube embedded in a micro-porous glass matrix (Figure 2a), the emission spectra of a single free standing MT exhibit very sharp periodic structure (Figure 3a). When separated from the matrix, the MT is much more optically dense than its surrounding medium allowing light propagating inside the MT to be spatially constrained to travel along the rim of a cross-section of the tube, and therefore it is said to be trapped in a WGMs. The presence of sharp emission peaks in the spectrum of a single MT is an immediate result of this optical confinement (Figure 3) These peaks correspond to optical resonance locations and reflect the fact that transition probabilities are increased for emission wavelengths near resonance.

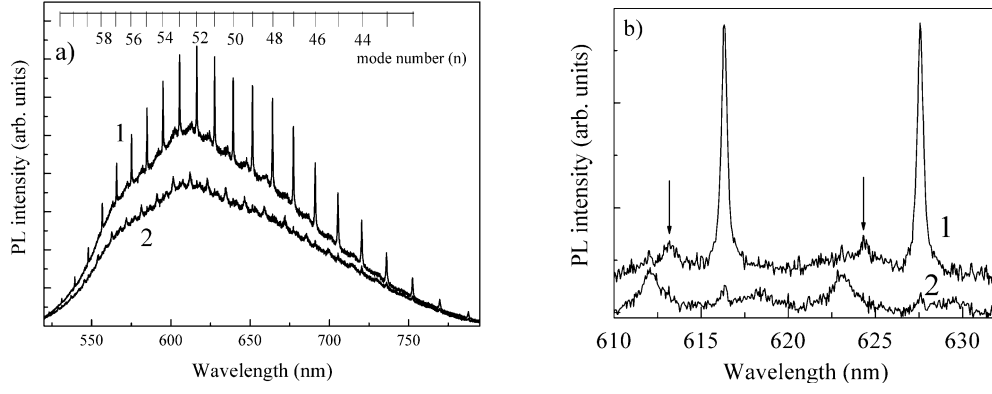


Figure 3. (a) Room-temperature micro-PL spectra of single free-standing microcavity with polarizer orientation parallel to the microtube axis (1) and polarizer rotated by  $90^\circ$  (2). (b) A region around  $TM_{52}$  WGM with subtracted PL background.

Due to the high quantum efficiency of the samples under study, the WGMs peaks are superimposed on a background signal arising from part of the emission which does not match any WGMs of the MT (Figure 3). The placement and spacing between WGMs peaks are determined by the diameter and refractive index of the microcavity while the spectral intensity distribution depends on the parameters of the emitting species and can be easily modified by doping of the original aluminosilicate gel, for example by rare earth ions. The most striking feature of the spectra presented in Figure 3 is the strong polarization properties. The sharp peaks dominating in the spectrum for a polarizer orientation parallel to the MT axis (Figure 3, curve 2) correspond to linear polarized light with the electric vector vibrating parallel to the axis of cylinder. Rotating the polarizer by  $90^\circ$  results in strong quenching of these WGMs (Figure 2, curve 3) unambiguously indicating their transverse magnetic (TM) character.

In order to identify peaks in observed WGMs structure, we have adopted the boundary-value solution to the problem of scattering of a plane electromagnetic waves by an dielectric microcylinder. For cylindrical symmetry the extinction efficiency is derivable from Lorenz-Mie theory when microcylinder is illuminated by monochromatic, plane polarized light with the electric vector vibrating parallel to the axis of cylinder (TM polarization):

$$Q_{ext}^{TM} = \frac{2}{x} \operatorname{Re} \left[ b_0 + 2 \sum_{n=1}^{\infty} b_n \right], \quad (1)$$

where  $x=2\pi r/\lambda$  is the size parameter,  $r$  is the radius of microcylinder,  $n$  is the angular mode number. Apart from  $n$  (which is proportional to the circumference of cross-section divided by the wavelength of the light propagating within the microcylinder), the spectral distributions of WGMs are characterized by the mode order  $l$  (which indicates the number of maxima in the radial distribution of the internal electric field), and the azimuthal mode number  $m$  (which gives the orientation of the WGMs orbital plane).

In the absence of gain, the Mie scattering partial wave amplitudes  $b_n(x,m)$  can be expressed in the form

$$b_n = \frac{mJ'_n(mx)J_n(x) - J_n(mx)J'_n(x)}{mJ'_n(mx)H_n^{(1)}(x) - J_n(mx)H_n^{(1)}(x)} \quad (2)$$

where  $J_n(x)$  is a Bessel function of the first kind,  $H_n(x)$  is a Hankel function of the second kind, and the primes denote differentiation of the functions with respect to their arguments. According to Eq. (1)-(2) resonance structure in scattering spectra can be expected as the real part of  $b_n$  reaches its maximum value of 1 and the imaginary part is passing through 0 from the positive to the negative side. In other words the resonances in the Mie scattering characteristics occur when denominators in Eq. (2) are equal to zero for a particular mode  $n$ .

These conditions are a transcendental equations, which can be solved for the size parameter  $x$  (position of a resonance) for given values of refractive index and for given mode number  $n$ . Thus comparing calculated results with the spectral positions of the WGMs in the experimental PL spectra we can identify the indexes  $n$  for each mode and estimate the diameter of the MT. The algorithm of the mode assignment can be as follows. 1) The resonant wavelengths corresponding WGMs resonances  $\lambda_i^{\text{exp}}$  ( $i = 1, 2 \dots, N$ ) are determined from a PL spectrum of single microtube. 2) We assume approximate value MT radius based on typical cross-sectional SEM image. 3) Theoretical resonance positions  $\lambda_i^{\text{theor}}$  are then calculated using eq. (2). 4) Two lists are compared and for each value of  $\lambda_i^{\text{exp}}$  the closest value  $\lambda_i^{\text{theor}}$  is suggested and difference between them  $\Delta_i$  is calculated. 5) Taking into account spectral resolution  $\Delta$  the correlation  $S = \frac{1}{N} \sum_1^N (1 + \Delta_i / \Delta)^{-1}$  is then maximized by adjusting only two fitting parameter, namely size of microcylinder and refractive index  $m$ . The results of the mode identification ( $TM_n^l$ ) for  $m = 1.48$  and  $D = 7.65 \mu\text{m}$  are shown in Figure 3a.

Subtraction of PL background (Figure 3b) allows us to reveal the presence of satellites: broader peaks of the same polarization, which are blue shifted with respect to the identified WGMs (indicated by arrows in Figure 3b). The separation between these satellites homogeneously increases with wavelength ranging between 8 and 18 nm and is identical to the WGMs spacings. Therefore the observed secondary structure cannot be attributed to the WGMs of higher  $l$ , for which smaller mode spacings are expected. Observation of two resonances of the same mode type can be explained by taking into account the fact that modes other than WGMs can be supported by the MT cavity. The presence of the second, inner surface has significant influence on the emission pattern of microcavity systems. As a result, the MT mode structure is more complex than in a single boundary microcavity.

If we fit the WGMs peaks by a Lorentzian function, we find quality factors defined by  $Q = \lambda_0 / \Delta\lambda$  ranging between 2000 and 3200 with the maximum  $Q$ -value obtained for the peak centered at 616 nm. The quality factor reflects how long a photon can be stored in the microcavity before leaking out. Therefore with knowledge of  $Q$  value, it is possible to estimate the average lifetime of photon in the relevant mode:  $\tau = Q / \omega_0$ , where  $\omega_0$  is the resonant frequency. In present sample this lifetime was found to be  $\sim 1$  ps for a WGMs of maximum  $Q$ -value. It is noteworthy, that the highest value of  $Q$ -factor ( $Q=3200$ ) recently defined in low-temperature (5K) micro-PL spectra of InGaAs-GaAs microtubes of 5  $\mu\text{m}$  diameter [8] is well comparable to our results which, however were obtained at room temperature. Apart from work by Kipp et al,[8] we were not able to find data published on WGMs structure in a spectra of micro-cylinders or micro-tubes with diameter comparable to present samples.

In our experiments at room temperature, no thermal degradation effects of the MT cavities caused by laser excitation have been found for increasing the pump power up to 0.22 mW. (Figure 4). It was found that the integrated PL intensity increases approximately linearly with excitation power up to 0.17 mW followed by a change in the slope. (Figure 4). However, we cannot take this as clear evidence of ASE, as we did not observe any mode narrowing in the spectral response.

The observation of a lasing or ASE threshold is problematic for three-dimensional microcavity structures in general. In the small volume limit as the fraction of spontaneous emission coupled to the cavity modes approaches unity, the light output from a microcavity becomes a nearly linear function of pump power, i.e. the laser or ASE threshold appears to vanish. However, apart from threshold intensity behavior and line narrowing there are other properties of the microcavity that are expected to clearly indicate transition to the regime of ASE. In order to understand the emission process further, we have studied the lifetime of the PL spectra of single MT as a function of intensity.

Table 2.

$I_{\text{ex}}$ ( $\mu\text{W}$ )	$\tau_1$ (ns)	$\alpha_1$	$\tau_2$ (ns)	$\alpha_2$	$\tau_3$ (ns)	$\alpha_3$	$\tau_{\text{av}}$ (ns)
0.03	1.757	0.29	5.605	0.52	11.983	0.19	7.86
55.3	0.968	0.40	3.671	0.47	9.281	0.13	5.39
0.03	1.622	0.29	5.364	0.51	12.041	0.20	7.98

The results presented in Figure 5 and Table 2 confirm that an increase of excitation power leads to an acceleration of the emission decay rate in the single MT cavity.

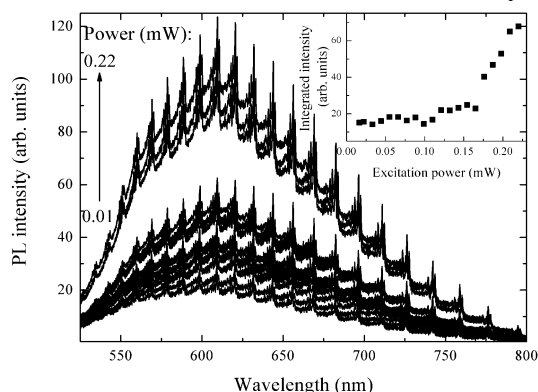


Figure 4. PL spectra of single microtube cavity at different pump powers. The inset shows the integrated PL intensity versus excitation power.

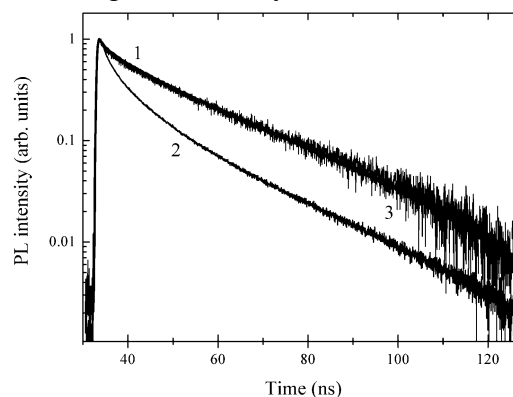


Figure 5. Time-dependent PL intensity decays of a single microtube detected at excitation power of 0.03  $\mu\text{W}$  (1), 55.3  $\mu\text{W}$  (2) and again 0.03  $\mu\text{W}$ .

level, the original PL decay characteristics are restored (Table 2). It is noteworthy that ASE is a highly nonlinear optical phenomenon. As a result, the PL decay observed at higher excitation power is much more non-exponential (judged by values of  $\chi^{(2)}$  (Table 2)) as compared with this detected in low-excitation regime (Figure 5). This fact along with clear decrease in PL lifetime (Figure 5, Table 2) lends strong credence to the occurrence of amplified spontaneous emission in a single microtube. The increased decay rate at high pump intensity unambiguously shows that we have achieved ASE from the microtube. This observation shows the high optical quality of these materials and that they have strong potential to act as microlasers.

**Abstract.** The authors studied the optical properties of a novel microtube cavity of  $\sim 8 \mu\text{m}$  diameter prepared by vacuum assisted filtration of aluminosilicate xerogel using micro-channel glass matrix followed by thermal treatment. Periodic very narrow peaks of the emission spectra corresponding to orthogonally polarized whispering gallery modes were detected.

## References

1. Vahala K.J. // Nature, 2003, V.424, N 6950, P.839.
2. Knight J.C., Driver H.S.T., Hutcheon R.J. // Opt. Lett., 1992, V. 17, N 18, P. 1280.
3. Moon H.-J., Chough Y.-T., An K. // Phys. Rev. Lett., 2000, V.85, N 15, P. 3161.
4. Shevchenko A., Lindfors K., Bucher C.K., Kaivola M. // Opt. Commun., 2005, V. 245, N 1-6, P. 349.
5. Wallingford R.A., Ewing A.G. // Anal. Chem., 1988, V. 60, P.1972.
6. Blair S., Chen Y. // Appl. Opt., 2001, V. 40, N 4, P. 570.
7. Hunter B.V., Bickel W.S. // Appl. Opt., 1994, V. 33, P. 8387.
8. Kipp T., Welsch H., Strelow C.H., Heyn C.H., Heitmann D. // Phys. Rev. Lett., 2006, V. 96, N 7, P. 077403.
9. Nogami M., Abe Y. // J. Non-Cryst. Solids, 1996, V. 197, N 1, P. 73.
10. Green W.H., Le K.P., Grey J., Au T.T., Sailor M.J. // Science, 1997, V. 276, P.1826.